Protein oligomerization modulates raft partitioning and apical sorting of GPI-anchored proteins

Simona Paladino,[1,2] Daniela Sarnataro,[1] Rudolf Pillich,[1] Simona Tivodar,[1] Lucio Nitsch,[1] and Chiara Zurzolo[1,2]

[1]Dipartimento di Biologia e Patologia Cellulare e Molecolare, Centro di Endocrinologia ed Oncologia Sperimentale, CNR, Università degli Studi di Napoli Federico II, Italy
[2]Unité de Trafic Membranaire et Pathogénèse, Institut Pasteur, 75105 Paris, France

An essential but insufficient step for apical sorting of glycosylphosphatidylinositol (GPI)-anchored proteins (GPI-APs) in epithelial cells is their association with detergent-resistant microdomains (DRMs) or rafts. In this paper, we show that in MDCK cells both apical and basolateral GPI-APs associate with DRMs during their biosynthesis. However, only apical and not basolateral GPI-APs are able to oligomerize into high molecular weight complexes. Protein oligomerization begins in the medial Golgi, concomitantly with DRM association, and is dependent on protein–protein interactions. Impairment of oligomerization leads to protein missorting. We propose that oligomerization stabilizes GPI-APs into rafts and that this additional step is required for apical sorting of GPI-APs. Two alternative apical sorting models are presented.

Introduction

The plasma membrane of polarized epithelial cells is divided into two domains, apical and basolateral, which display different protein and lipid composition therefore resulting in specialized functions (Rodriguez-Boulan and Powell, 1992; Mostov et al., 2003). This asymmetric molecular distribution depends on continuous sorting of newly synthesized components and their regulated internalization (Mellman, 1996; Matter, 2000; Nelson and Yeaman, 2001). Intracellular sorting may occur at the level of the TGN where, upon recognition of specific apical or basolateral sorting signals (Matter and Mellman, 1994; Mostov et al., 2000), proteins following a direct route to the plasma membrane are segregated into distinct vesicles and separately delivered to the apical or basolateral surface (Wandinger-Ness et al., 1990; Rodriguez-Boulan and Powell, 1992; Keller et al., 2001; Kreitzer et al., 2003). It has been postulated that sphingolipid- and cholesterol-rich microdomains (rafts) can act as sorting platforms for inclusion of proteins into apical post-TGN sorting vesicles (Simons and Ikonen, 1997) because of their capacity to segregate specific classes of lipids and proteins (Simons and van Meer, 1988; Brown and London, 1998). By using Triton X-100 (TX-100) and other nonionic detergents at 4°C, rafts can indeed be extracted as detergent-resistant microdomains (DRMs) containing different apical membrane proteins.

Glycosylphosphatidylinositol (GPI)-anchored proteins (GPI-APs) are apically sorted in several epithelial cell lines (Brown et al., 1989; Lisanti et al., 1989) and use their GPI anchor to associate with rafts. It has therefore been proposed that the GPI anchor acts as an apical sorting determinant by mediating raft association (Simons and van Meer, 1988; Simons and Ikonen, 1997). However, the roles of the GPI anchor and the lipid rafts as apical determinants have been recently questioned by the findings that not only Fisher rat thyroid cells (Zurzolo et al., 1993; Lipardi et al., 2000), but also MDCK cells can sort GPI-APs both to the apical and basolateral domains (Benting et al., 1999b; McGwire et al., 1999; Sarnataro et al., 2002).

We have analyzed the DRM association of four GPI-APs that are differently sorted in MDCK cells: GFP-GPI (a simple reporter protein made of GFP fused to the GPI anchor attachment signal from the folate receptor) and placental alkaline phosphatase (PLAP), which are apically sorted, and growth hormone-decay accelerating factor (GH-DAF; in which the rat growth hormone is fused to the GPI attachment signal of DAF) and the native prion protein, PrP, that are basolateral. We show here that both apical and basolateral GPI-APs are associated with DRMs indicating that lipid rafts do not provide an exclusive mechanism for driving apical sorting. We also found that only the apically sorted GPI-APs are able to form high molecular weight (HMW) complexes. Oligomerization of apical GPI-APs occurs during the transport to the plasma membrane and is concomitant with raft association. Depletion of cholesterol, which impairs raft association and apical sorting, also affects the oli-

Figure 1. **GPI-APs are apically and basolaterally sorted.** MDCK cells stably expressing GFP-GPI, PLAP, PrP, or GH-DAF were grown to confluence on filters. Cells were fixed and in the case of PLAP, PrP, and GH-DAF stained with specific antibodies followed by a TRITC-conjugated secondary antibody in nonpermeabilized conditions. Serial confocal sections were collected from the top to the bottom of cell monolayers (A). Cells were labeled with LC-biotin respectively added to the apical or the basolateral surface. After immunoprecipitation with specific antibodies samples were run on SDS-PAGE and revealed using HRP-streptavidin (B). The histograms show percentages of apical or basolateral protein expressed as the average of three different experiments. Standard error bars are indicated.
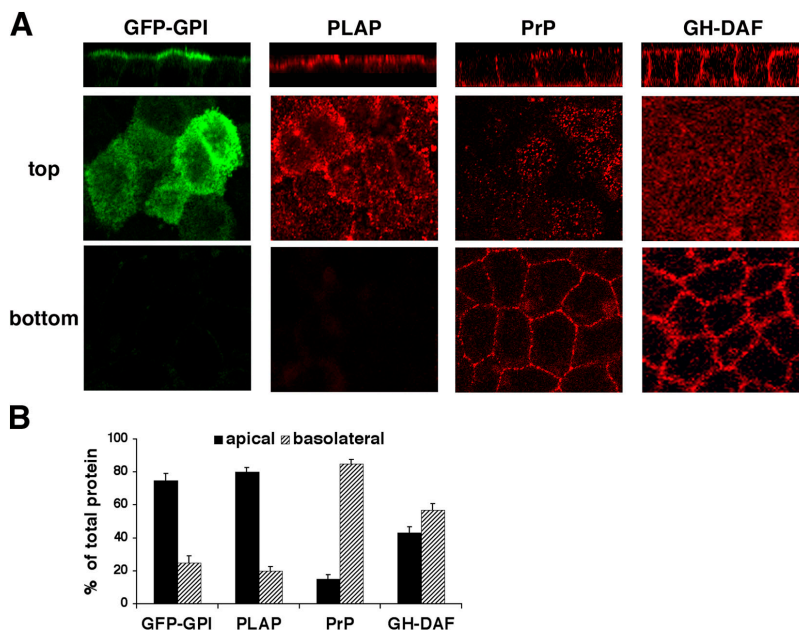
gomerization rate of apical GPI-APs in the Golgi. Finally, impairment of oligomerization leads to protein missorting to the basolateral domain. We propose that by increasing raft affinity oligomerization promotes GPI-APs stabilization into rafts and that this additional step is necessary for GPI-APs apical sorting.

Results

Different GPI-APs are differently sorted in MDCK cells

The majority of GPI-APs are apically sorted in several epithelial cell lines (Brown et al., 1989; Lisanti et al., 1989). One exception is the Fisher rat thyroid cell line which can sort GPI-APs both to apical and basolateral domains (Zurzolo et al., 1993; Lipardi et al., 2000). Furthermore, we and others (Benting et al., 1999b; McGwire et al., 1999; Sarnataro et al., 2002) recently found that some GPI-APs are also sorted to the basolateral surface in MDCK cells. To better understand the mechanism of sorting of GPI-APs we therefore studied four different GPI-APs transfected in MDCK cells: two chimeric GPI-APs (GFP-GPI and GH-DAF) and two native GPI-APs (PLAP and PrP), which were shown previously to be differently sorted in MDCK cells.

By confocal microscopy (Fig. 1 A) and surface biotinylation (Fig. 1 B) we confirmed that GFP-GPI and PLAP were predominantly enriched on the apical surface, whereas PrP and GH-DAF were mainly localized on the basolateral membrane (Arreaza and Brown, 1995; Benting et al., 1999b; Sarnataro et al., 2002; Polishchuk et al., 2004).

Apical and basolateral GPI-APs are DRM associated

It has been postulated that in MDCK cells GPI-APs are sorted to the apical surface through their incorporation into lipid microdomains (rafts) in the Golgi complex (Simons and Ikonen,

1997). Rafts can be isolated from whole cells as membranes resistant to extraction in cold nonionic detergents (detergent resistant membrane [DRM]) such as TX-100 (Edidin, 2003; Helms and Zurzolo, 2004; Simons and Vaz, 2004). To understand the role of DRM association for apical sorting of GPI-APs we extracted the different MDCK clones expressing GFP-GPI, PLAP, PrP, and GH-DAF in cold TX-100, as described previously (Brown and Rose, 1992; Zurzolo et al., 1994). We found that both apical and basolateral GPI-APs were insoluble to TX-100 extraction (respectively, ~75–80% for the apical proteins and ~60–70% for the basolateral ones; Fig. 2 A). Because TX-100 insolubility can also result from events other than DRM association (Low and Saltiel, 1988; Brown and Rose, 1992), we purified TX-100 insoluble microdomains by centrifugation to equilibrium on sucrose density gradients, that allows the segregation of lipid-rich components from the bulk of TX-100 insoluble material (Brown and Rose, 1992). Consistently with the TX-100 extraction results (Fig. 2 A) we found that all four GPI-APs floated to the DRM-GM1–enriched fractions (4–7) of the gradients (Fig. 2 B). Therefore, these experiments clearly confirmed that association to DRMs is not sufficient to dictate apical sorting (Benting et al., 1999b; Lipardi et al., 2000; Sarnataro et al., 2002).

Moreover, it is interesting to note that there is a difference in the isopycnic density of the gradient fractions reached by apical and basolateral GPI-APs. Although GFP-GPI and PLAP were recovered maximally in fraction 5, PrP and GH-DAF were maximally enriched in heavier fractions (Fig. 2 B). Furthermore, we found higher amounts of apical GPI-APs in DRMs compared with the basolateral proteins. The average of five different experiments showed that for both apical proteins ~75% was found in DRM fractions (4–7) in contrast to only ~40–45% for the basolateral proteins. These differences in fraction density and in the amount of protein floating is not due to a different lipid profile of the gradients from the different stably
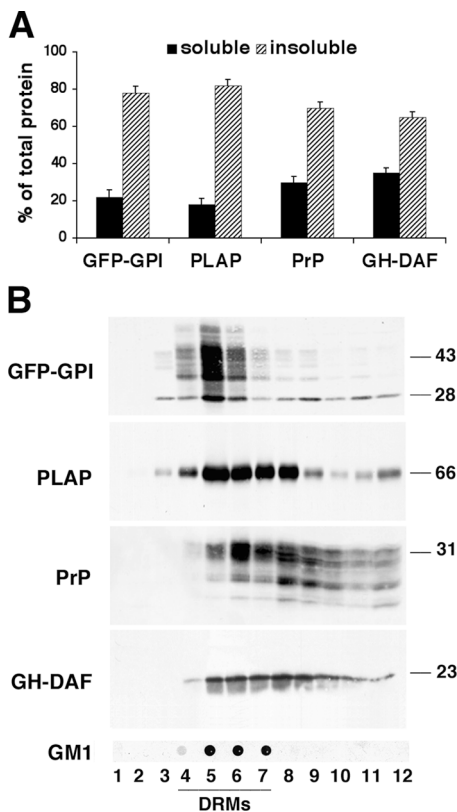
Figure 2. **Both apical and basolateral GPI-APs associate with DRM.** MDCK cells stably expressing GFP-GPI, PLAP, PrP, or GH-DAF were lysed in TNE/TX-100 buffer at 4°C and separated by centrifugation into soluble and insoluble fractions (A) or run through 5–40% sucrose gradients (B). Fractions of 1 ml were collected from top (fraction 1) to bottom (fraction 12) after centrifugation to equilibrium (B). After TCA precipitation samples were run on SDS-PAGE and detected by specific antibodies. An aliquot of each fraction was spotted on the nitrocellulose membrane and GM1 was revealed using cholera toxin conjugated to HRP. The histograms in A show the percent of soluble or insoluble protein from three different experiments (standard error bars are indicated). Note that the slower mobility band (43 kD) detected for GFP-GPI is specific for GFP because it is not present in untransfected cells (unpublished data) and it was described previously as a partially denatured GFP dimer (Inouye and Tsuji, 1994). PrP migrates as four major bands: the mature fully glycosylated form corresponding to the molecular mass of 31 kD, the immature glycosylated forms (diglycosylated and monoglycosylated) and the unglycosylated form (Sarnataro et al., 2002, 2004).

transfected clones because endogenous GM1 was similarly enriched in fractions 4–7 in all tested cell lines (unpublished data).

Only apical GPI-APs form HMW complexes both at steady state and at the plasma membrane

The differences in DRM association observed for apical and basolateral GPI-APs could be due to a different lipid environment surrounding the different proteins or to a different affinity for DRMs of apical and basolateral GPI-APs. In the latter case a high affinity could lead to a more stable association of the protein with lipid rafts which could promote apical sorting. Hence, it has been shown that clustering of seven or fewer GPI-APs increases their raft association and this leads to their rerouting to late endosomes instead of recycling endosomes

(Fivaz et al., 2002). Because it is well known that protein multimers partition preferentially in DRMs compared with their monomeric form (Fivaz et al., 2002; Cunningham et al., 2003; Helms and Zurzolo, 2004; Simons and Vaz, 2004), we decided to analyze the oligomerization state of the different apical and basolateral GPI-APs by sedimentation on velocity gradients (where the proteins sediment according to their molecular weight) after extraction in SDS/TX-100 buffer (Scheiffele et al., 1998). Although ~20–30% of GFP-GPI and ~25–35% of PLAP were purified as HMW complexes containing more than a trimer, both PrP and GH-DAF were purified almost exclusively from the gradient fractions corresponding to their expected monomeric molecular weights (Fig. 3). Therefore, these experiments revealed that only apical GPI-APs are in oligomeric complexes.

To rule out the possibility that these HMW complexes were formed as a consequence of detergent addition to the cells we used a different approach in native conditions. Therefore, we added a chemical cross-linking agent, bis(sulfosuccinimidyl)suberate (BS3), that is able to cross-link molecules that are in very close proximity (arm length, 11.4 Å; Friedrichson and Kurzchalia, 1998) either to the apical or the basolateral surface of filters grown cells. As expected, we did not find HMW complexes in the absence of cross-linking (Fig. 4). However, when cells expressing GFP-GPI were chemically cross-linked at 4°C from the apical surface, a smear between ~80 and ~300 kD was detected on the gel (Fig. 4). Similarly, we detected a band corresponding to a relative molecular mass of 120 kD (dimer), a band of 180 kD (trimer), and a smear at higher molecular weights after apical cross-linking of PLAP-expressing cells (Fig. 4). In contrast, neither PrP nor GH-DAF were found in cross-linked complexes when BS3 was added to the basolateral surface (Fig. 4). Because BS3 is membrane impermeable, our data indicate that apical GPI-APs are in cross-linkable complexes at the cell surface, whereas basolateral ones are not.

These results, obtained with two very different approaches, clearly indicate that only apical GPI-APs are clustered. In addition, they show that the capability to form HMW complexes is not a simple consequence of being in rafts (shared by both apical and basolateral GPI-APs), but appears to be an exclusive characteristic of apically sorted GPI-APs. The next question is whether this feature has a role in their apical sorting.

Oligomer formation occurs during passage through the Golgi concomitantly with DRM association

To study when and where apical GPI-APs were oligomerizing during their life span and to understand whether this event had any role in apical sorting, we analyzed the kinetics of GPI-APs oligomerization by pulse-chase experiments (Fig. 5, left). Although we obtained overlapping data for GFP-GPI and PLAP, we only show the oligomer formation of PLAP (Fig. 5) because it is glycosylated and therefore it was possible to monitor its passage through the Golgi apparatus by acquisition of resistance to endoglycosidase H (Endo H) digestion (Kornfeld and Kornfeld, 1985). After a brief pulse of 10 min with

Figure 3. **Only apical GPI-APs form HMW complexes.** MDCK cells stably expressing GFP-GPI, PLAP, PrP, or GH-DAF were lysed in buffer containing 0.4% SDS and 0.2% TX-100 and run through a nonlinear 5–30% sucrose gradient. Fractions of 500 μl were collected from the top (fraction 1) to the bottom (fraction 9) of the gradients. Proteins were TCA precipitated and detected by Western blotting using specific antibodies. The molecular weight of the monomeric forms of each protein is indicated. The position on the gradients of molecular weight markers is indicated on the top of the panel. Distribution curves of the average of three different experiments (standard error bars are indicated) are shown in the right panel.
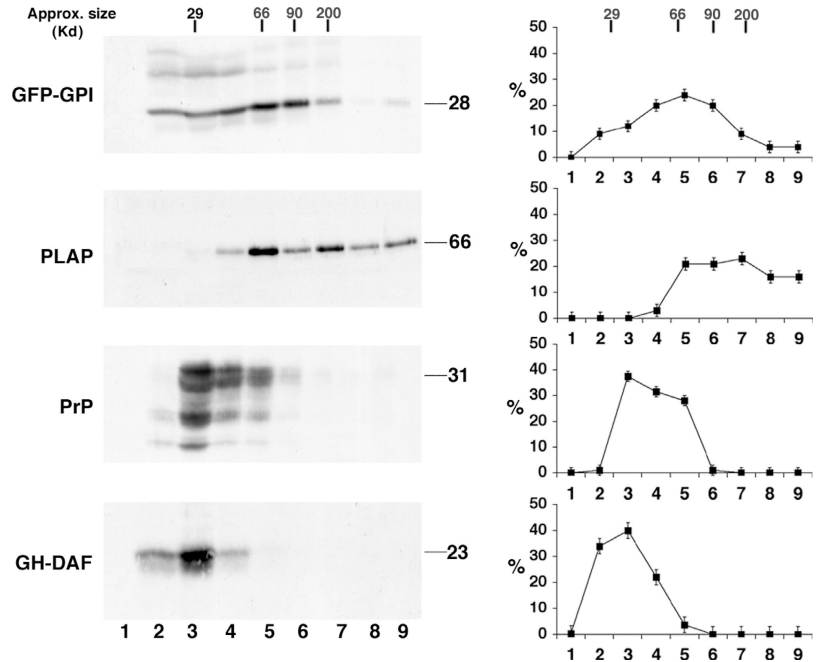
[^{35}S]met/cys, cells were chased for the indicated times, lysed in SDS/TX-100 containing buffer, and run on velocity gradients (Fig. 5, left). PLAP began to form HMW complexes after 20 min of chase when a portion of the protein had acquired Endo H resistance (therefore after the medial Golgi). After 40 min of chase, when almost all PLAP was Endo H resistant, ~30% of the protein was found in HMW complexes (Fig. 5, top left). Interestingly, PLAP was recovered in HMW complexes (although in lower amounts, ~20%) also after 80 min of chase, i.e., when the majority of the protein had already reached the plasma membrane, as shown by our targeting assays (Fig. S1 A, available at http://www.jcb.org/cgi/content/full/jcb.200407094/DC1). Our results are in agreement with previous data (Friedrichson and Kurzchalia, 1998; Harder et al., 1998; Varma and Mayor, 1998) showing that GPI-APs are in clusters at the cell surface, in addition they demonstrate that apical GPI-APs cluster during their passage through the Golgi where sorting is supposed to occur (Wandinger-Ness et al., 1990; Rodriguez-Boulan and Powell, 1992; Mostov et al., 2000; Keller et al., 2001).

To understand whether there was any correlation between oligomerization and association to DRMs we analyzed the kinetics of DRM association of PLAP and GFP-GPI (not depicted) at the same chase times on flotation gradients (Fig. 5, top right). Both apical GPI-APs began to associate with DRMs at the same time that they began to oligomerize. Indeed by 40 min of chase, PLAP was associated to DRMs and was in HMW complexes (Fig. 5, top right). These data demonstrate that the two phenomena are concomitant and suggest that they might be connected. As a control, we repeated the same experiment for the two basolateral proteins that are DRM associated but do not oligomerize. We show only PrP because suitable for the Endo H assay. As expected, PrP did not oligomerize during its passage through the Golgi and migrated almost exclusively as a monomer on the velocity gradient during all chase times (Fig. 5,

bottom left). Nonetheless, the mature highly glycosylated form of PrP (H) began to associate with DRMs at 20-min chase time and remained DRM associated after 40 and 80 min of chase similarly to PLAP (Fig. 5, compare top with bottom right). Interestingly, the diglycosylated immature isoform of PrP (D) was recovered in DRM fractions already after 10 min of chase (when the protein is in the ER). This is a specific feature of PrP and we recently demonstrated that this early rafts association is important for the correct folding of the protein (Sarnataro et al., 2004).

In conclusion these results demonstrate that both apical and basolateral GPI-APs associate with DRM fractions during their passage through the Golgi, therefore excluding the possi-
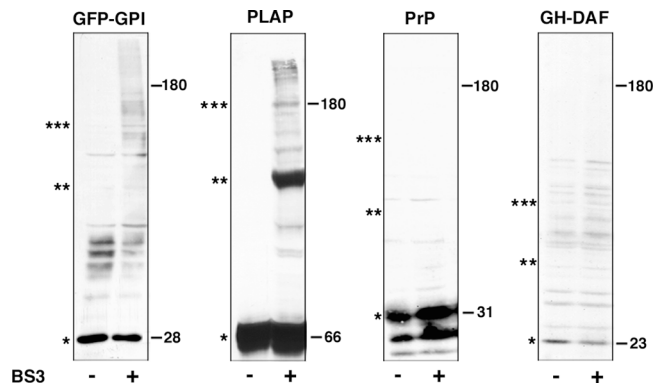
Figure 4. **Only apical GPI-APs can be cross-linked at the cell surface.** MDCK cells stably expressing GFP-GPI, PLAP, PrP, or GH-DAF grown on filters were incubated with BS3 (0.5 mM). After lysis, proteins were TCA precipitated, run on SDS-PAGE (in a 6–12% gradient gel for GFP-GPI, PrP, or GH-DAF or 8% gel for PLAP) in reducing conditions and revealed with specific antibodies. The molecular weight of the monomeric forms (*) of each protein is indicated, together with the position of a 180-kD marker. ** and *** indicate, respectively, the expected molecular weight of the dimeric and trimeric forms of each protein.

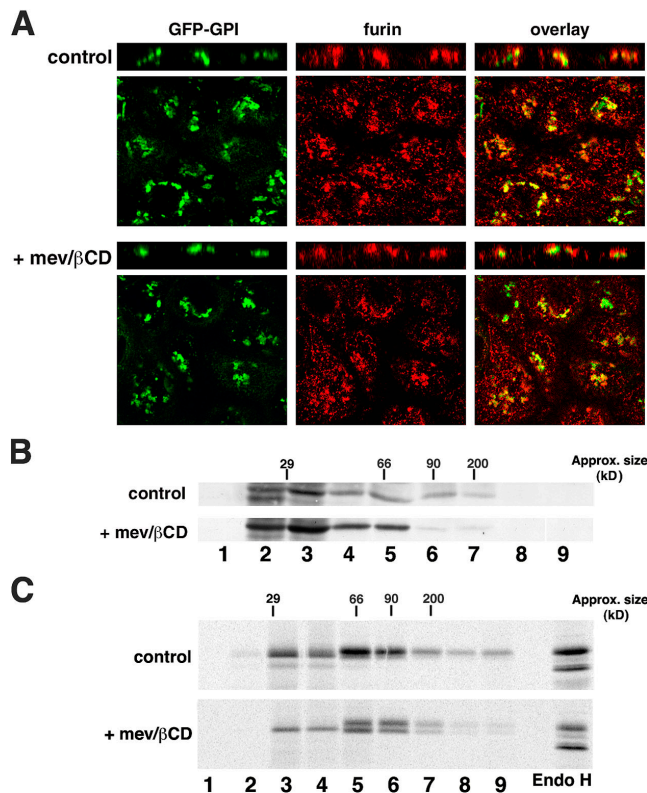**PLAP**   **velocity gradients**   **floatation gradients**

PrP
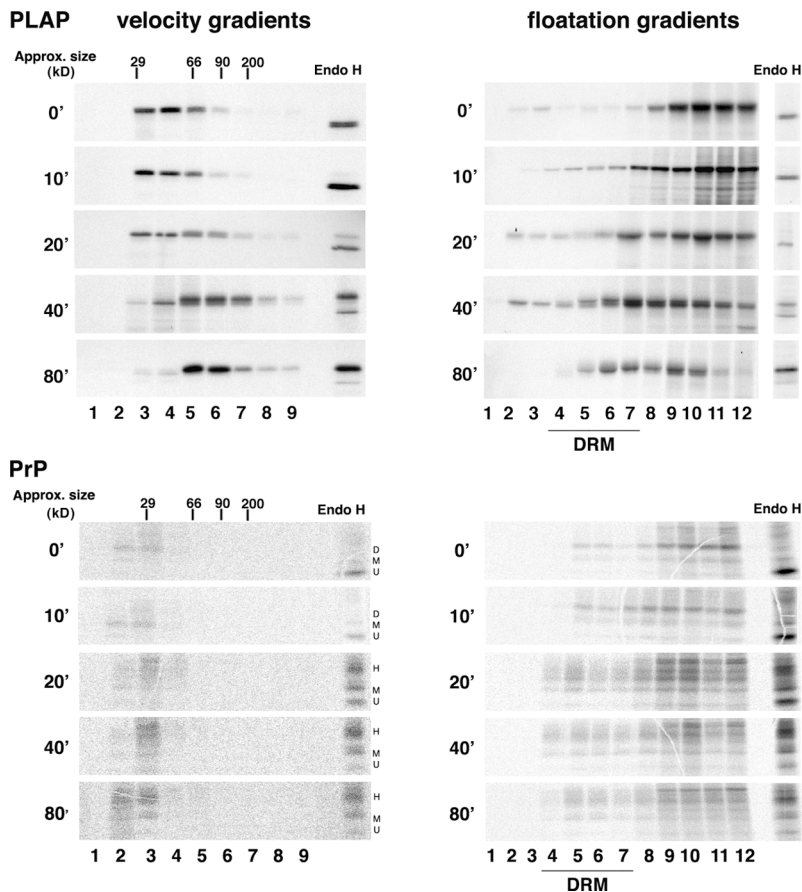
Figure 5. **HMW complex formation occurs concomitantly with DRM association of the protein.** MDCK cells expressing PLAP or PrP grown on plastic dishes were pulsed for 10 min with [^{35}S]cys and -met and chased for the indicated times. At the end of each chase time the cells were lysed and purified on velocity gradients (left) or on sucrose density gradients (right). For each chase time an aliquot of lysate was immunoprecipitated and treated with Endo H. H, mature highly glycosylated; D, diglycosylated; M, monoglycosylated; U, unglycosylated PrP isoforms (Sarnataro et al., 2002, 2004). Note that up to 10 min of chase PLAP was not found in HMW complex, by 20 and 40 min of chase ∼10% and ∼25–30%, respectively, of PLAP was in HMW complex. At 80 min PLAP was still in these complexes (∼15–20%). In contrast, all PrP was purified exclusively as monomer form at all chase times. White lines indicate that intervening lanes have been spliced out.

bility that the different sorting was due to the lack of raft association of basolateral GPI-APs in this compartment. We also show that concomitantly with DRM association only apical GPI-APs oligomerize in HMW complexes.

Cholesterol depletion affects HMW complex formation

The concomitance of oligomerization and DRM association during passage of the protein through the late Golgi prompted us to evaluate whether the two events were linked by a cause–effect relation. To understand whether association to rafts was necessary for oligomer formation we impaired DRM association by depleting the cells of cholesterol (Keller and Simons, 1998; Lipardi et al., 2000) and analyzed oligomer formation in these conditions. In each experiment we obtained a depletion of 50–55% of the intracellular cholesterol using a combined treatment with mevinolin and methyl-β-cyclodextrin (βCD; see Materials and methods). As already shown for other GPI-APs, cholesterol depletion impairs both raft association and apical sorting of PLAP and GFP-GPI (Fig. S2, available at http://www.jcb.org/cgi/content/full/jcb.200407094/DC1). However, as described previously (Lee et al., 2002) it was difficult to see any effect on oligomeric complex formation at steady state because the proteins were already complexed in HMW complexes at the time of the treatment (unpublished data). Therefore, we analyzed the effect of cholesterol depletion on the oligomeric state of the protein in the Golgi apparatus, where

oligomerization occurs and should be maximal (Fig. 5). To accumulate proteins in the TGN, control and cholesterol depleted cells expressing GFP-GPI were subjected to a temperature block at 19.5°C in the presence of cycloheximide. By double immunofluorescence with furin convertase (Liu et al., 1997) we found that GFP-GPI is highly enriched in the TGN, as shown previously (Polishchuk et al., 2004), in both control and cholesterol depleted cells (Fig. 6 A). We then subjected the cell lysates to velocity gradients and found that the ratio between the monomeric and oligomeric forms changed dramatically in cholesterol-depleted cells compared with control cells (Fig. 6 B). We observed a sevenfold decrease of the oligomeric form and a consequent increase of the monomeric form in cholesterol-depleted cells (Fig. 6 B). Because the TGN block was not tight enough for PLAP we repeated the pulse-chase and velocity gradient experiments shown in Fig. 5, but after cholesterol depletion (Fig. 6 C). As shown by the 40-min chase time point in Fig. 6 C, cholesterol depletion also affects PLAP oligomerization during its passage through the late Golgi apparatus. This suggests that rafts constitute a favorable environment for HMW complex formation of apical GPI-APs and that this event occurs during the passage of the protein through the late Golgi. Both temperature block and cholesterol depletion did not have any effect on the oligomerization of basolateral GPI-APs in that they did not oligomerize in any of these conditions (Fig. S3, available at http://www.jcb.org/cgi/content/full/jcb.200407094/DC1).

A

GFP-GPI | furin | overlay

control

+ mev/βCD

B

29 66 90 200   Approx. size (kD)

control

+ mev/βCD

1 2 3 4 5 6 7 8 9

C

29 66 90 200   Approx. size (kD)

control

+ mev/βCD

1 2 3 4 5 6 7 8 9   Endo H

Figure 6. **Cholesterol depletion affects HMW complex formation in the Golgi.** Cells expressing GFP-GPI (A and B) or PLAP (C) were treated or not (control) with mevinolin (mev) and βCD to deplete the cells of cholesterol. Control and cholesterol-depleted cells (+ mev/βCD) expressing GFP-GPI were subjected to a temperature block in the TGN, fixed, and stained with an antibody against furin followed by a TRITC-conjugated secondary antibody. xz and xy images acquired with a confocal microscope show colocalization of GFP-GPI with the TGN marker in both control and cholesterol depleted cells (A). Control and cholesterol-depleted cells (+ mev/βCD) expressing GFP-GPI were lysed and run through a nonlinear 5–30% sucrose velocity gradient as in Fig. 3 B (B). Control and cholesterol depleted cells (+ mev/βCD) expressing PLAP were pulsed for 10 min with [³⁵S]met, chased for 40 min and purified on velocity gradients. An aliquot of lysate was immunoprecipitated and treated with Endo H as in Fig. 5 (C).

Mutations that impair GFP-GPI oligomerization affect its apical sorting

To understand whether GPI-APs clustering in HMW complexes has a key role in their apical sorting, we decided to impair oligomerization and study its effect on apical sorting. It was recently described that GFP oligomerizes in the secretory pathway and that GFP oligomers depend on disulphide bonds (Jain et al., 2001). Because two specific cysteines, cys 49 and cys 71, are involved in GFP oligomerization (Jain et al., 2001), we mutated them in the GFP-GPI construct by site-directed mutagenesis. In contrast to the wild-type, the double cys GFP-GPI mutant (S49/71) ran exclusively as a monomer in both nonreducing gels (Fig. 7 A) and on velocity gradients (Fig. 7 B) both at steady state (top) and after the block in the TGN (bottom) indicating that it was not able to oligomerize. However, similar to the wild-type protein, ~70% of the S49/71 mutant was TX-100 insoluble (unpublished data) and ~60% floated to the lighter fractions on sucrose density gradients (Fig. 7 C), although there was a shift toward the bottom of the

gradient of the mutated protein compared with the wild-type (compare Fig. 2 B with Fig. 7 C). Thus the two point mutations do not affect GFP-GPI association with DRMs, suggesting that they did not dramatically alter the structure of the protein (because it was immunoprecipiated with similar affinity as the wild-type protein (Fig. S4, available at http://www.jcb.org/cgi/content/full/jcb.200407094/DC1) nor impair its transport to the plasma membrane, as shown below (Fig. 7 D).

To analyze whether impairment of oligomerization of a DRM-associated protein had an effect on its apical sorting we analyzed the distribution of the S49/71 mutant on the plasma membrane. By confocal microscopy, using an antibody against c-Myc (or anti GFP; unpublished data) added to the top or the bottom of the filter-grown monolayers in nonpermeabilized conditions, we were able to analyze exclusively the signal from the surface localized proteins. As shown by xz and xy sections (Fig. 7 D, left), whereas wild-type GFP-GPI is exclusively apical, the S49/71 mutant is missorted and is localized both on the apical and basolateral surfaces. These results were confirmed by a surface biotinylation assay (Fig. 7 D, right) and therefore show that impairment of oligomerization dramatically affects GFP-GPI apical delivery and leads to missorting.

Discussion

A model for the apical sorting of GPI-APs has been proposed in which closely packed lipid microdomains (rafts) assembled within the fluid bilayer of the TGN act as sorting platforms for inclusion of cargo proteins destined for delivery to the apical membrane (Simons and Ikonen, 1997). However, many reports show that raft association is not sufficient for apical sorting of GPI-APs. The protein ectodomain has been suggested to have a predominant role in the apical sorting of GPI-APs either through N- or O-linked sugars (Benting et al., 1999b) or because of an as yet undefined conformation-dependent signal (Benting et al., 1999b; Rodriguez-Boulan and Gonzalez, 1999; Lipardi et al., 2000; Helms and Zurzolo, 2004).

In this paper, we have analyzed the role of rafts in GPI-APs sorting by studying the behavior of different apically and basolaterally sorted GPI-APs in MDCK cells. We found that both apical (GFP-GPI and PLAP) and basolateral (PrP and GH-DAF) GPI-APs are DRM associated (Figs. 1 and 2). These data confirm previous findings that partitioning into lipid rafts of GPI-APs depends on the specific affinity of the long and saturated acyl chains of the GPI anchor for the sphingolipid-enriched rafts environment (Brown and London, 1998; Benting et al., 1999a; Lipardi et al., 2000; Mayor and Riezman, 2004). They also clearly demonstrate, as proposed previously (Benting et al., 1999b; Lipardi et al., 2000; Sarnataro et al., 2002), that raft association is not sufficient to determine apical sorting of GPI-APs. Interestingly, we found that apical GPI-APs were more insoluble in TX-100 than the basolateral ones and floated to lower isopycnic density on sucrose gradients (Fig. 2, A and B). These differences could be explained in two different ways: either apical and basolateral GPI-APs partition with different lipid microdomains, as recently shown for two different GPI-APs extracted from brain, Thy-1 and PrP (Brugger et al.,
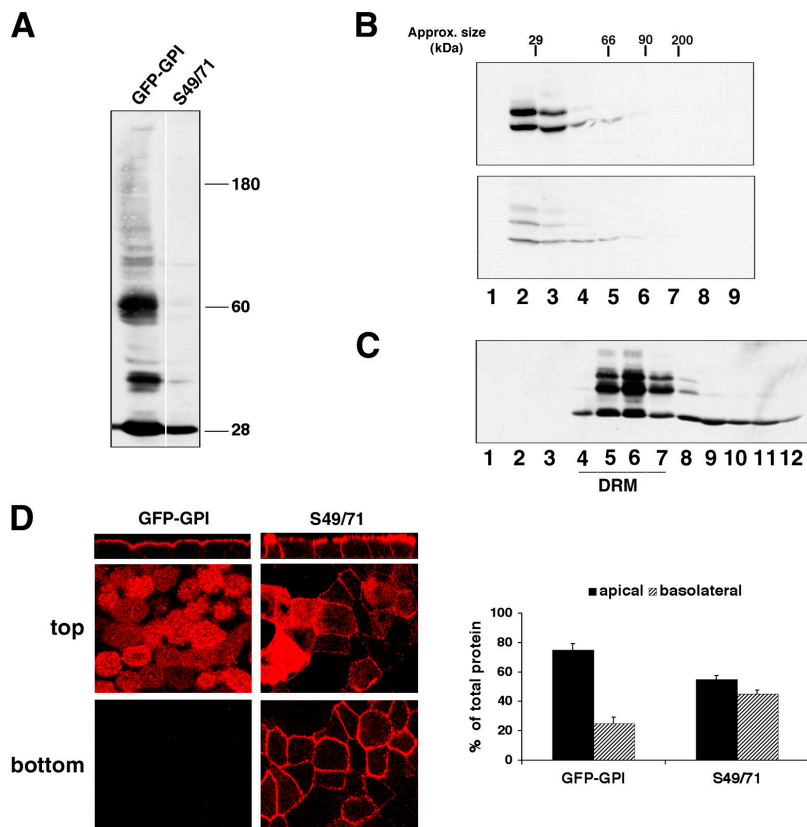
Figure 7. **Oligomerization impairment leads GFP-GPI missorting.** MDCK cells expressing GFP-GPI or the double cysteine GFP-GPI mutant (S49/71) were lysed in TNE/TX-100 buffer and samples were run on SDS-PAGE in nonreducing conditions. Although GFP-GPI migrates as monomeric and HMW forms, the S49/71 mutant runs exclusively as a monomer (A). White lines indicate that intervening lanes have been spliced out. (B) MDCK cells expressing the S49/71 mutant of GFP-GPI were purified on velocity gradients at the steady state (top) and after temperature block in the TGN (bottom). After TCA precipitation the protein was revealed in the different fractions by Western blotting using an anti-GFP antibody. Also in this assay the mutant migrates almost exclusively as a monomer. MDCK cells expressing S49/71 mutant of GFP-GPI were lysed in TNE/TX-100 buffer at 4°C and subjected to flotation by centrifugation to equilibrium on sucrose gradients as described before. The collected fractions were TCA precipitated and proteins were revealed using an antibody against GFP (C). (D) MDCK cells expressing wild-type and double cysteine mutant of GFP-GPI were grown on filters in polarized conditions for 4 d and stained using an antibody against c-Myc in nonpermeabilizing conditions followed by a TRITC-conjugated secondary antibody. Images were collected with a confocal microscope. xy images shown are taken at the top or at the bottom of the cells (left). xz images are also shown in top left panels. Filter grown cells were biotinylated as in Fig. 1 B. The histograms show percentages of apical or basolateral protein expressed as the average of three different experiments. Standard error bars are indicated (right).

2004), or apical and basolateral GPI-APs have different affinities for lipid rafts.

Because confinement of GPI-APs into lipid microdomains is a transient phenomenon (Sheets et al., 1997; Dietrich et al., 2001; Zurzolo et al., 2003; Simons and Vaz, 2004), residency time in rafts could be a mechanism that dictates the different sorting. This hypothesis has been previously validated in the case of GPI-APs sorting in the endosomal compartment where higher raft affinity determines sorting to lysosomes rather than to recycling endosomes (Fivaz et al., 2002). Similarly, in yeast the missorting to the vacuole of a mutant of the plasma membrane proton ATPase pump Pma1P (Pma 1-7) is restored by expression of Ast1p (a peripheral membrane protein), which promotes Pma 1-7 partitioning into rafts (Bagnat et al., 2001). Another suggestion is that affinity for rafts can be modulated by the oligomeric state of the protein (Helms and Zurzolo, 2004; Simons and Vaz, 2004). For example the GPI-linked protein uPAR partitions into rafts as a dimer but not as a monomer (Cunningham et al., 2003), whereas aereolysin-clustered GPI-APs have a higher affinity for rafts than their monomers (Fivaz et al., 2002). Based on these findings we decided to analyze the oligomeric state of apical and basolateral GPI-APs in MDCK cells and surprisingly found, using two different approaches, that only apical GPI-APs were in HMW complexes (Figs. 3 and 4) and that this occurred before delivery to the surface, during passage through the Golgi apparatus (Fig. 5).

By running flotation gradients at the same time as velocity gradients in pulse-chase experiments we also show that oligomerization and DRM association of apical GPI-APs occur

concomitantly (Fig. 5). Because cholesterol depletion, which affects GPI-APs DRM association (Fig. S2), also impairs protein oligomerization in the Golgi apparatus and in the TGN (Fig. 6, B and C), these experiments indicate that the two events are linked by a cause–effect relation. Similarly, Sharma and colleagues (Sharma et al., 2004) have found that in living cells cluster organization of GPI-APs is mediated by cholesterol and that the ratio of monomers to clusters increases in cholesterol depleted cells.

Oligomerization of secreted proteins has been shown to play a key role in sorting (Huttner et al., 1991; Reaves and Dannies, 1991). Moreover, it has been proposed that aggregation of either proteins or lipids acts as a general sorting signal for protein and lipid targeting to exosomes (Vidal et al., 1997). Similarly, oligomerization could be a necessary mechanism to sort GPI-APs to the apical surface (Zurzolo et al., 2003; Helms and Zurzolo, 2004). To test this hypothesis we impaired oligomerization of GFP-GPI by mutating the two cysteine residues known to be important (Jain et al., 2001). Significantly, we found that the mutated form did not oligomerize (Fig. 7, A and B) and was completely missorted (Fig. 7 D). These data indicate that impairment of oligomerization also impairs apical delivery. Furthermore, the fact that oligomer formation occurs concomitantly with DRM association (Fig. 5) suggests that oligomerization and association to lipid rafts cooperate to promote apical sorting.

We propose that oligomerization could promote stabilization of the GPI-APs into rafts leading to their incorporation into apical vesicles. On the contrary GPI-APs monomers hav-

ing a shorter residency time in rafts would be excluded from apical vesicles. Alternatively protein oligomerization could drive the coalescence of small rafts into a larger raft which would increase the curvature of the membrane (Harder et al., 1998; Roper et al., 2000; Huttner and Zimmerberg, 2001; Ikonen, 2001; Edidin, 2003) and result in the budding of an apical vesicle (Fig. 8, model).

Interestingly, some years ago Edidin and colleagues (Hannan et al., 1993) showed that the newly arrived molecules of gD1-DAF at the apical surface of MDCK cells were less mobile than long-term resident molecules, suggesting that GPI-APs were clustered before their delivery to the apical surface. On the contrary in mutant Con A-resistant MDCK cells, that fail to sort GPI-APs to the apical membrane, they found that newly delivered basolateral gD1-DAF molecules were not immobilized, even though they were still associated with DRMs (Zurzolo et al., 1994). These data are entirely consistent with our findings and suggest that basolateral missorting of GPI-APs in this mutant cell line is not due to lack of DRM association, but to lack of clustering and stabilization into rafts which occurs before arrival at the plasma membrane.

Therefore, we propose that oligomerization and raft association cooperate in promoting apical sorting during the passage of GPI-APs through the Golgi apparatus (Fig. 5), most likely in the TGN (Fig. 6). These conclusions are in conflict with a recent publication (Polishchuk et al., 2004) which showed that in MDCK cells GFP-GPI is sorted to the apical surface via an indirect route, suggesting that sorting between apical and basolateral proteins probably occurs after proteins have reached the basolateral plasma membrane (Polishchuk et al., 2004). In direct contrast we show here by targeting assays (Fig. S1) that both GFP-GPI and PLAP are directly sorted to the apical surface in MDCK cells. Although we cannot formally exclude that by this assay we are missing a rapid passage to the basolateral surface, the bulk of our data does not support this explanation. In addition it should be noted that in the Polishchuk et al. (2004) paper it is clearly shown by immunofluorescence and immunoelectron microscopy that apical and basolateral proteins were already segregated into distinct domains in the TGN emerging tubules. In the light of these observations our data could infer that a clustering mechanism based on oligomerization and raft association segregates apical GPI-APs from basolateral proteins in the TGN and that they subsequently travel in the same post-TGN carrier to the basolateral surface. However, whereas basolateral proteins would rapidly diffuse into this membrane domain, clustered apical GPI-APs would be rapidly endocytosed and redirected to the apical surface. This is nonetheless unlikely because GPI-APs internalization is a rather slow process (for review see Mayor and Riezman, 2004). We believed that the discrepancy between the data could lie in the different methods used and in the cell culture conditions. We have shown previously that during the establishment of the polarized monolayer in filter culture, apical proteins normally sorted via a direct route can use the transcytotic pathway (Zurzolo et al., 1992), therefore all our experiments were performed in fully polarized conditions after 4 d of confluent growth on filters.
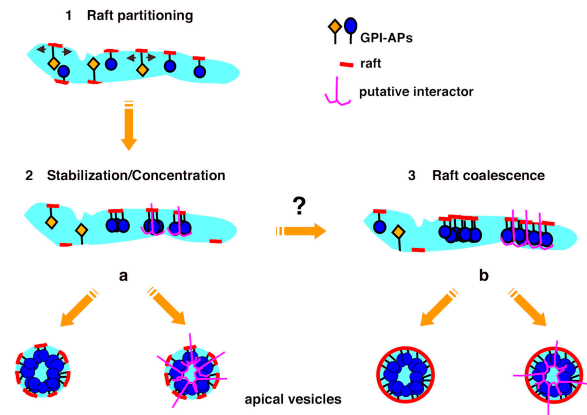
Figure 8. **Multistep model for apical sorting of GPI-APs in polarized epithelial cells.** (1) Raft partitioning. Both apical and basolateral GPI-APs partition with rafts due to chemical affinity of the GPI-APs for rafts. (2) Stabilization/Concentration. Only apical GPI-APs are stabilized into rafts by protein oligomerization, increasing their raft affinity. A putative apical receptor could be involved in this second step. (3) Raft coalescence. Protein oligomerization could lead to coalescence of more rafts with consequent formation of a functional larger raft from which apical vesicles bud. Two alternative mechanisms leading to the formation of apical vesicles are presented: (a) oligomerization/stabilization into rafts is sufficient to drive apical sorting; and (b) oligomerization drives coalescence of more rafts and subsequent formation of an apical vesicle.

What does oligomerization depend on? GPI proteins can interact with other molecules via the lipid anchor, via the protein ectodomain, or by both. Hence, lipid–lipid, glycan–lipid, protein–lipid, and protein–protein interactions could determine oligomerization. The fact that depletion of cholesterol reduces oligomer formation in the TGN suggests that lipid rafts are a favorable environment for oligomers to form. However, once oligomers are formed they are independent of rafts, and they resist conditions (e.g., SDS extraction) in which DRMs are disrupted. Therefore, protein–protein interactions might have a predominant role in stabilizing the HMW complex. Although in the case of GFP-GPI we found the involvement of disulphide bonds, weak noncovalent interactions between protein ectodomains are most likely to be responsible for the clustering of native GPI-APs in the proper raft environment. We indeed found that HMW complexes of PLAP were sensitive to heat, but not to reducing agents (unpublished data) indicating that the oligomerization process is protein specific and is mediated by homotypic interactions. In support of this hypothesis preliminary data indicate that PLAP and GFP-GPI are not in the same HMW complex, i.e., they do not coimmunoprecipitate when coexpressed in MDCK cells (Fig. S5, available at http://www.jcb.org/cgi/content/full/jcb.200407094/DC1). Another possibility that we cannot exclude is that a putative interactor present in rafts, like Ast1p in yeast (Bagnat et al., 2001), could recognize specific signals in the apical GPI-APs and favor their clustering (Fig. 8). This interactor could be a lectin that recognizes N- or O-glycans, as proposed previously (Fiedler and Simons, 1995; Benting et al., 1999b) or it could recognize a three-dimensional structure in the protein or lipid moiety (Rodriguez-Boulan and Gonzalez, 1999).

In all these scenarios oligomerization would be the prime mechanism determining apical sorting. Alternatively, HMW complex formation may simply be a consequence of the concentration/stabilization of the proteins into rafts during inclusion into apical vesicles, for example, by different affinities of different GPI anchors for rafts. However, this seems unlikely because we would not expect that impairment of oligomerization (as a simple consequence of protein packing in rafts) would lead to protein missorting. A careful analysis of anchor structure, DRM composition and HMW complex content will nonetheless be required to fully answer these questions. Notwithstanding, it is clear that at least two requirements are necessary for apical sorting of GPI-APs: the first one is partitioning into rafts, the second is clustering and stabilization into rafts. Only the proteins fulfilling both these requirement will be apically sorted (Fig. 8).

Materials and methods

Reagents and antibodies
Cell culture reagents were purchased from GIBCO BRL. Antibodies were purchased from the following companies: polyclonal αGFP was purchased from CLONTECH Laboratories, Inc.; monoclonal αGFP was purchased from Molecular Probes; αPLAP was purchased from Rockland; αGH was purchased from Biotrend GMBH; α-cmyc and α-SAF 32 αPrP were purchased from Cayman Chemical; and biotin, HRP-linked streptavidin and BS3 were purchased from Pierce Chemical Co. All other reagents were purchased from Sigma-Aldrich.

Cell culture and transfections
MDCK cells were grown in DME containing 5% FBS. MDCK cells were transfected with sequences encoding GFP-GPI and GH-DAF as described previously (Zurzolo et al., 1993). The GFP-GPI construct was a gift from S. Lacey (Southwestern University, Georgetown, TX) and was constructed in the eukaryotic expression vector pJB20. It has an EcoRI site at the 5′ end, a HindIII site at the 3′ end and a PstI site that separates the ecto and anchor domains. In addition it has an myc tag at the NH_2 terminus and contains an ER import signal. GH-DAF cDNA was a gift from T. Kurzchalia (Max Planck Institute, Dresden, Germany). Stable clones were selected by resistance to neomycin. PLAP and PrP expressing cells were described previously (Lipardi et al., 2000; Sarnataro et al., 2002).

Site-directed mutagenesis
The mutant form of GFP-GPI (single and double cysteine mutants) were obtained by site-directed mutagenesis using the QuickChange II XL site-directed mutagenesis kit (Stratagene). The oligonucleotides used for the mutations were: 49 cys 5′ (5′-CCCTGAAGTTCAGTACCACCGGCAAGC-3′) and 49 cys 3′ (5′-GCTTGCCGGTGGTACTGATGAACTTCAGGG-3′) to change ser 49 in cys; and 71 cys 5′ (5′-ACCTACGGCGTGCAGAGC-TTCAGCCGCTACCCC-3′) and 71 cys 3′ (5′-GGGGTAGCGGCTGAA-GCTCTGCACGCCGTAGGT-3′) to change ser 71 in cys. The double mutant was obtained using as template the cDNA containing the 49 or 71 cys mutations for a second round of mutagenesis to introduce the other mutation.

Fluorescence microscopy
MDCK cells were grown on transwell filters for 3–4 d, washed with PBS containing $CaCl_2$ and $MgCl_2$, fixed with 4% PFA, and quenched with 50 mM NH_4Cl. Depending on the experiment, cells were permeabilized with 0.075% saponin. Primary antibodies were detected with TRITC-conjugate secondary antibodies. Images were collected using a laser scanning confocal microscope (LSM 510; Carl Zeiss MicroImaging, Inc.) equipped with a planapo 63× oil-immersion (NA 1.4) objective lens.

Biotinylation assay
Cells grown on transwell filters were selectively biotinylated and processed as described previously (Zurzolo et al., 1994). Lysates were immunoprecipitated with specific antibodies and run on SDS-PAGE. Biotinylated GFP-GPI, PLAP, PrP, and GH-DAF were revealed by HRP-conjugated streptavidin.

TX-100 extraction and sucrose density gradients
Cells that had just reached confluency in dishes were lysed for 20 min on ice in 1 ml of TNE (Tris, NaCl, EDTA)/TX-100 buffer (25 mM Tris-HCl, pH 7.5, 150 mM NaCl, 5 mM EDTA, 1% TX-100) and centrifuged at 14,000 rpm in a microfuge (Beckman Coulter) for 2 min at 4°C. Supernatants, representing the soluble material, were removed and the pellets were solubilized in 100 μl of solubilization buffer (50 mM Tris-HCl, pH 8.8, 5 mM EDTA, 1% SDS). DNA was sheared through a 22-g needle. Supernatants were adjusted to 0.1% SDS before TCA precipitation (Brown and Rose, 1992).

Sucrose gradient analysis of TX-100–insoluble material was performed using previously published protocols (Brown and Rose, 1992; Zurzolo et al., 1994). After lysis in TNE/1% TX-100 buffer on ice, cells were scraped from dishes, brought to 40% sucrose, and placed at the bottom of a centrifuge tube. A discontinuous sucrose gradient (5–35% in TNE) was layered on top of the lysates and the samples were centrifuged at 39,000 rpm for 18 h in an ultracentrifuge (model SW41; Beckman Coulter). One ml fractions were harvested from the top of the gradient and TCA precipitated. In both cases samples were revealed by Western blotting using specific antibodies.

To reveal the distribution of GM1 in the gradient 30 μl of each fraction (before TCA precipitation) were spotted on nitrocellulose filters and detected with HRP-conjugated cholera toxin B subunit (Sigma-Aldrich).

Velocity gradients
Velocity gradients were performed using previously published protocols (Scheiffele et al., 1998). Cells were grown to confluency in 100 mm dishes, washed in PBS containing $CaCl_2$ and $MgCl_2$ and lysed on ice for 30 min in 20 mM Tris, pH 7.4, 100 mM NaCl, 0.4% SDS, 0.2% TX-100. Lysates were scraped from dishes, sheared through a 26-g needle and layered on top of a sucrose gradient (30–5%) after nuclei pelleting. After centrifugation at 45,000 rpm for 16 h in an ultracentrifuge (model SW50; Beckman Coulter), fractions of 500 μl were harvested from the top of the gradient and TCA precipitated. Proteins were revealed by Western blotting using specific antibodies.

Pulse chase
Cells grown in 100 mm dishes were starved of methionine and cysteine for 1 h, and pulse labeled for 10 min with medium containing 100 μCi/ml of Pro-mix ^{35}S-cell labeling (Amersham Biosciences) and incubated in chase medium (DME containing 5% FBS and met/cys 10×) for different times.

Endo H digestion
Digestion with Endo H was performed on immunoprecipitated materials. The antigen–antibody complexes were removed from sepharose beads using 50 μl of 0.1 M Na citrate/0.1% SDS and boiling for 3 min. Samples were incubated with 5 mU of Endo H for 16 h at 37°C. Samples were run on SDS-PAGE and revealed by fluorography.

Cholesterol depletion
To deplete the cells of cholesterol we used a previously described protocol (Keller and Simons, 1998; Lipardi et al., 2000). Briefly MDCK cells were plated on filters and mevinolin (10 μM) was added to the cells 24 h after plating in DME supplemented with 5% dilipidated calf serum and mevalonate (250 μM). After 48 h of this treatment, βCD (10 mM) was added in medium containing 20 mM Hepes, pH 7.5, and 0.2% bovine albumin for 1 h at 37°C. To determine the rate of cholesterol depletion we measured cholesterol cellular levels by a colorimetric assay. In brief, cells were washed twice with PBS containing $CaCl_2$ and $MgCl_2$, lysed with appropriate lysis buffer and infinity cholesterol reagent (Sigma-Aldrich) was added to the lysates in the ratio 1:10. Absorbance of samples was read at 550 nm.

Temperature block
To achieve an almost complete protein block in the TGN we modified a previously published protocol (Toomre et al., 1999). Cells grown on filters for 3 or 4 d were incubated at 19.5°C for 2 h in areal medium (F12 Coon's modified medium without $NaHCO_3$ and with BSA 0.2% and 20 mM Hepes, pH 7.4). In the last hour at 19.5°C they were treated with cycloheximide (150 μg/ml).

Cross-linking
0.5 mM BS3 was added to the cells grown on dishes for 45 min and quenched for 15 min with 20 mM Tris, pH 7.5, as described elsewhere (Friedrichson and Kurzchalia, 1998). Proteins were TCA precipitated, separated on SDS-PAGE, and revealed by specific antibodies.

References

Arreaza, G., and D.A. Brown. 1995. Sorting and intracellular trafficking of a glycosylphosphatidylinositol-anchored protein and two hybrid transmembrane proteins with the same ectodomain in Madin-Darby canine kidney epithelial cells. *J. Biol. Chem.* 270:23641–23647.

Bagnat, M., A. Chang, and K. Simons. 2001. Plasma membrane proton ATPase Pma1p requires raft association for surface delivery in yeast. *Mol. Biol. Cell.* 12:4129–4138.

Benting, J., A. Rietveld, I. Ansorge, and K. Simons. 1999a. Acyl and alkyl chain length of GPI-anchors is critical for raft association in vitro. *FEBS Lett.* 462:47–50.

Benting, J.H., A.G. Rietveld, and K. Simons. 1999b. N-Glycans mediate the apical sorting of a GPI-anchored, raft-associated protein in Madin-Darby canine kidney cells. *J. Cell Biol.* 146:313–320.

Brown, D.A., and J.K. Rose. 1992. Sorting of GPI-anchored proteins to glycolipid-enriched membrane subdomains during transport to the apical cell surface. *Cell.* 68:533–544.

Brown, D.A., and E. London. 1998. Functions of lipid rafts in biological membranes. *Annu. Rev. Cell Dev. Biol.* 14:111–136.

Brown, D.A., B. Crise, and J.K. Rose. 1989. Mechanism of membrane anchoring affects polarized expression of two proteins in MDCK cells. *Science.* 245:1499–1501.

Brugger, B., C. Graham, I. Leibrecht, E. Mombelli, A. Jen, F. Wieland, and R. Morris. 2004. The membrane domains occupied by glycosylphosphatidylinositol-anchored prion protein and Thy-1 differ in lipid composition. *J. Biol. Chem.* 279:7530–7536.

Cunningham, O., A. Andolfo, M.L. Santovito, L. Iuzzolino, F. Blasi, and N. Sidenius. 2003. Dimerization controls the lipid raft partitioning of uPAR/CD87 and regulates its biological functions. *EMBO J.* 22:5994–6003.

Dietrich, C., Z.N. Volovyk, M. Levi, N.L. Thompson, and K. Jacobson. 2001. Partitioning of Thy-1, GM1, and cross-linked phospholipid analogs into lipid rafts reconstituted in supported model membrane monolayers. *Proc. Natl. Acad. Sci. USA.* 98:10642–10647.

Edidin, M. 2003. The state of lipid rafts: from model membranes to cells. *Annu. Rev. Biophys. Biomol. Struct.* 32:257–283.

Fiedler, K., and K. Simons. 1995. The role of N-glycans in the secretory pathway. *Cell.* 81:309–312.

Fivaz, M., F. Vilbois, S. Thurnheer, C. Pasquali, L. Abrami, P.E. Bickel, R.G. Parton, and F.G. van der Goot. 2002. Differential sorting and fate of endocytosed GPI-anchored proteins. *EMBO J.* 21:3989–4000.

Friedrichson, T., and T.V. Kurzchalia. 1998. Microdomains of GPI-anchored proteins in living cells revealed by crosslinking. *Nature.* 394:802–805.

Hannan, L.A., M.P. Lisanti, E. Rodriguez-Boulan, and M. Edidin. 1993. Correctly sorted molecules of a GPI-anchored protein are clustered and immobile when they arrive at the apical surface of MDCK cells. *J. Cell Biol.* 120:353–358.

Harder, T., P. Scheiffele, P. Verkade, and K. Simons. 1998. Lipid domain structure of the plasma membrane revealed by patching of membrane components. *J. Cell Biol.* 141:929–942.

Helms, J.B., and C. Zurzolo. 2004. Lipids as targeting signals: lipid rafts and intracellular trafficking. *Traffic.* 5:247–254.

Huttner, W.B., H.H. Gerdes, and P. Rosa. 1991. The granin (chromogranin/secretogranin) family. *Trends Biochem. Sci.* 16:27–30.

Huttner, W.B., and J. Zimmerberg. 2001. Implications of lipid microdomains for membrane curvature, budding and fission. *Curr. Opin. Cell Biol.* 13:478–484.

Ikonen, E. 2001. Roles of lipid rafts in membrane transport. *Curr. Opin. Cell Biol.* 13:470–477.

Inouye, S., and F.I. Tsuji. 1994. Aequorea green fluorescent protein. Expression of the gene and fluorescence characteristics of the recombinant protein. *FEBS Lett.* 341:277–280.

Jain, R.K., P.B. Joyce, M. Molinete, P.A. Halban, and S.U. Gorr. 2001. Oligomerization of green fluorescent protein in the secretory pathway of endocrine cells. *Biochem. J.* 360:645–649.

Keller, P., and K. Simons. 1998. Cholesterol is required for surface transport of influenza virus hemagglutinin. *J. Cell Biol.* 140:1357–1367.

Keller, P., D. Toomre, E. Diaz, J. White, and K. Simons. 2001. Multicolour imaging of post-Golgi sorting and trafficking in live cells. *Nat. Cell Biol.* 3:140–149.

Kornfeld, R., and S. Kornfeld. 1985. Assembly of asparagine-linked oligosaccharides. *Annu. Rev. Biochem.* 54:631–664.

Kreitzer, G., J. Schmoranzer, S.H. Low, X. Li, Y. Gan, T. Weimbs, S.M. Simon, and E. Rodriguez-Boulan. 2003. Three-dimensional analysis of post-Golgi carrier exocytosis in epithelial cells. *Nat. Cell Biol.* 5:126–136.

Lee, M.C., S. Hamamoto, and R. Schekman. 2002. Ceramide biosynthesis is required for the formation of the oligomeric H+-ATPase Pma1p in the yeast endoplasmic reticulum. *J. Biol. Chem.* 277:22395–22401.

Lipardi, C., L. Nitsch, and C. Zurzolo. 2000. Detergent-insoluble GPI-anchored proteins are apically sorted in fischer rat thyroid cells, but interference with cholesterol or sphingolipids differentially affects detergent insolubility and apical sorting. *Mol. Biol. Cell.* 11:531–542.

Lisanti, M.P., I.W. Caras, M.A. Davitz, and E. Rodriguez-Boulan. 1989. A glycophospholipid membrane anchor acts as an apical targeting signal in polarized epithelial cells. *J. Cell Biol.* 109:2145–2156.

Liu, G., L. Thomas, R.A. Warren, C.A. Enns, C.C. Cunningham, J.H. Hartwig, and G. Thomas. 1997. Cytoskeletal protein ABP-280 directs the intracellular trafficking of furin and modulates proprotein processing in the endocytic pathway. *J. Cell Biol.* 139:1719–1733.

Low, M.G., and A.R. Saltiel. 1988. Structural and functional roles of glycosylphosphatidylinositol in membranes. *Science.* 239:268–275.

Matter, K. 2000. Epithelial polarity: sorting out the sorters. *Curr. Biol.* 10:R39–R42.

Matter, K., and I. Mellman. 1994. Mechanisms of cell polarity: sorting and transport in epithelial cells. *Curr. Opin. Cell Biol.* 6:545–554.

Mayor, S., and H. Riezman. 2004. Sorting GPI-anchored proteins. *Nat. Rev. Mol. Cell Biol.* 5:110–120.

McGwire, G.B., R.P. Becker, and R.A. Skidgel. 1999. Carboxypeptidase M, a glycosylphosphatidylinositol-anchored protein, is localized on both the apical and basolateral domains of polarized Madin-Darby canine kidney cells. *J. Biol. Chem.* 274:31632–31640.

Mellman, I. 1996. Endocytosis and molecular sorting. *Annu. Rev. Cell Dev. Biol.* 12:575–625.

Mostov, K.E., M. Verges, and Y. Altschuler. 2000. Membrane traffic in polarized epithelial cells. *Curr. Opin. Cell Biol.* 12:483–490.

Mostov, K., T. Su, and M. ter Beest. 2003. Polarized epithelial membrane traffic: conservation and plasticity. *Nat. Cell Biol.* 5:287–293.

Nelson, W.J., and C. Yeaman. 2001. Protein trafficking in the exocytic pathway of polarized epithelial cells. *Trends Cell Biol.* 11:483–486.

Polishchuk, R., A. Di Pentima, and J. Lippincott-Schwartz. 2004. Delivery of raft-associated, GPI-anchored proteins to the apical surface of polarized MDCK cells by a transcytotic pathway. *Nat. Cell Biol.* 6:297–307.

Reaves, B.J., and P.S. Dannies. 1991. Is a sorting signal necessary to package proteins into secretory granules? *Mol. Cell. Endocrinol.* 79:C141–C145.

Rodriguez-Boulan, E., and A. Gonzalez. 1999. Glycans in post-Golgi apical targeting: sorting signals or structural props? *Trends Cell Biol.* 9:291–294.

Rodriguez-Boulan, E., and S.K. Powell. 1992. Polarity of epithelial and neuronal cells. *Annu. Rev. Cell Biol.* 8:395–427.

Roper, K., D. Corbeil, and W.B. Huttner. 2000. Retention of prominin in microvilli reveals distinct cholesterol-based lipid micro-domains in the apical plasma membrane. *Nat. Cell Biol.* 2:582–592.

Sarnataro, D., S. Paladino, V. Campana, J. Grassi, L. Nitsch, and C. Zurzolo. 2002. PrPC is sorted to the basolateral membrane of epithelial cells independently of its association with rafts. *Traffic.* 3:810–821.

Sarnataro, D., V. Campana, S. Paladino, M. Stornaiuolo, L. Nitsch, and C. Zurzolo. 2004. PrPC association with lipid rafts in the early secretory pathway stabilizes its cellular conformation. *Mol. Biol. Cell.* 15:4031–4042.

Scheiffele, P., P. Verkade, A.M. Fra, H. Virta, K. Simons, and E. Ikonen. 1998. Caveolin-1 and -2 in the exocytic pathway of MDCK cells. *J. Cell Biol.*

140:795–806.

Sharma, P., R. Varma, R.C. Sarasij, Ira, K. Gousset, G. Krishnamoorthy, M. Rao, and S. Mayor. 2004. Nanoscale organization of multiple GPI-anchored proteins in living cell membranes. *Cell.* 116:577–589.

Sheets, E.D., G.M. Lee, R. Simson, and K. Jacobson. 1997. Transient confinement of a glycosylphosphatidylinositol-anchored protein in the plasma membrane. *Biochemistry.* 36:12449–12458.

Simons, K., and E. Ikonen. 1997. Functional rafts in cell membranes. *Nature.* 387:569–572.

Simons, K., and G. van Meer. 1988. Lipid sorting in epithelial cells. *Biochemistry.* 27:6197–6202.

Simons, K., and W.L. Vaz. 2004. Model systems, lipid rafts, and cell membranes. *Annu. Rev. Biophys. Biomol. Struct.* 33:269–295.

Toomre, D., P. Keller, J. White, J.C. Olivo, and K. Simons. 1999. Dual-color visualization of trans-Golgi network to plasma membrane traffic along microtubules in living cells. *J. Cell Sci.* 112:21–33.

Varma, R., and S. Mayor. 1998. GPI-anchored proteins are organized in submicron domains at the cell surface. *Nature.* 394:798–801.

Vidal, M., P. Mangeat, and D. Hoekstra. 1997. Aggregation reroutes molecules from a recycling to a vesicle-mediated secretion pathway during reticulocyte maturation. *J. Cell Sci.* 110:1867–1877.

Wandinger-Ness, A., M.K. Bennett, C. Antony, and K. Simons. 1990. Distinct transport vesicles mediate the delivery of plasma membrane proteins to the apical and basolateral domains of MDCK cells. *J. Cell Biol.* 111:987–1000.

Zurzolo, C., G. van Meer, and S. Mayor. 2003. The order of rafts. Conference on microdomains, lipid rafts and caveolae. *EMBO Rep.* 4:1117–1121.

Zurzolo, C., A. Le Bivic, A. Quaroni, L. Nitsch, and E. Rodriguez-Boulan. 1992. Modulation of transcytotic and direct targeting pathways in a polarized thyroid cell line. *EMBO J.* 11:2337–2344.

Zurzolo, C., M.P. Lisanti, I.W. Caras, L. Nitsch, and E. Rodriguez-Boulan. 1993. Glycosylphosphatidylinositol-anchored proteins are preferentially targeted to the basolateral surface in Fischer rat thyroid epithelial cells. *J. Cell Biol.* 121:1031–1039.

Zurzolo, C., W. van't Hof, G. van Meer, and E. Rodriguez-Boulan. 1994. VIP21/caveolin, glycosphingolipid clusters and the sorting of glycosylphosphatidylinositol-anchored proteins in epithelial cells. *EMBO J.* 13:42–53.